S Y N O P S I S

of

The Ph.D. Thesis Entitled

SYNTHESIS AND OPTICAL PROPERTIES OF STRONTIUM PYROPHOSPHATE PHOSPHOR

Submitted For The Degree

of

DOCTOR OF PHILOSOPHY

By

NIMESH PRAFULBHAI PATEL

Under the guidance of

Dr. M. SRINIVAS

Department of Physics
Faculty of Science
The M. S. University of Baroda, Vadodara

February–2017

INTRODUCTION

Rare earth doped inorganic luminescent materials are well known for the emission at distinct wavelengths in the electromagnetic spectrum. The luminescent materials are called as the phosphor. The phosphors have wide range of applications in the lighting devices such as cathode ray tubes (CRT), tri-phosphor fluorescent lamps, x-ray intensifying screens and newly developed vacuum mercury-free lamps. It has other applications in display such as plasma display panels and field emission displays [1]. The momentous application of phosphors for light emitting diodes (LEDs) technology changes the history of the solid state lighting and has completely changed the "world of luminance". LEDs are significantly energy-efficient lighting device with long lifetime.

A luminescent phosphor is a solid, which converts certain types of energy into electromagnetic radiation over and above thermal radiation. The electromagnetic radiation emitted by a luminescent phosphor is usually ranging in between the UV to the IR wavelength range. The luminescence from the phosphors can acquire by exciting the phosphor in different manners such as by UV and visible radiation (photoluminescence), by a beam of energetic electrons (cathodoluminescence), by x-rays (x-ray excited luminescence), etc. Thermoluminescence is one of the distinct way to get luminescence, which is stimulation by the heating of luminescence, preliminary excited in a different way.

Luminescence measures the energy levels of the luminescence centers formed inside the phosphors. The energy level of a luminescence center is defined as its characteristic state, which is related to the physical nature of the center and to the energetic and dynamic processes that the center undergoes. The ground state is defined as the state with the lowest energy. States of higher energy are called excited states. A center possesses several distinct reservoirs of energy levels, including electronic, vibrational, rotational, transitional, and those associated with nuclear and electron spin. In luminescence phosphors, the energy levels of interest are those that are associated with electronic and vibrational transitions [2].

Several research groups had done research to study its optical properties. D. Hou, et al. reported photoluminescence of Ce^{3+} at two different sites in α-$Sr_2P_2O_7$ under vacuum UV and x-ray excitation synthesize by solid state reaction method [3]. V. Natarajan, et al. reported photoluminescence, thermally stimulated luminescence (TSL) and electron paramagnetic resonance of europium-ion doped strontium pyrophosphate synthesize by chemical precipitation method. TSL study was illustrated after gamma irradiation of samples by Co^{60} source [4]. A. N. Yazici, et al. reported thermoluminescent properties of $Sr_2P_2O_7$ doped with copper, rare earth elements synthesize by solid state reaction method. TL study was carried out after beta irradiation for various dose [5]. Z. Hao, et al. reported white light emitting diode by using α-$Ca_2P_2O_7$: Eu^{2+}, Mn^{2+} phosphor synthesize by solid state reaction method [6]. Z. Hao, et al. reported phase dependent photoluminescence and energy transfer in $Ca_2P_2O_7$: Eu^{2+}, Mn^{2+} phosphors for white LEDs synthesize by solid state reaction

method [7]. R. Kohale, et al. reported Synthesis and luminescent properties of Ce^{3+} doped $SrCaP_2O_7$ phosphor by modified solid state diffusion technique [8].

The investigation of the scientific literature survey of the pyrophosphate phosphors, it is found that all research groups had studied photoluminescence properties of different inorganic pyrophosphates. Very few research groups had been studied the photoluminescence and thermoluminescence after irradiation properties together of rare earth doped strontium pyrophosphate. In this research, I have synthesized rare earth doped strontium pyrophosphate phosphor to study photoluminescence (PL), thermoluminescence (TL) and structural properties of phosphor. Concentration of doping dependent PL and TL study was done for different rare earth doped phosphors. TL study of the phosphors was analysed by X-ray and beta irradiation for various doses. This research work carried out the predominant applications of strontium pyrophosphate in the TL dosimetry, LED and solid state lighting.

MOTIVATIONS

Rare earth activated inorganic pyrophosphate phosphor materials have generated enormous interest and considerable attention because of their easy synthesis processes, low cost, chemical and thermal stabilities, and low environmental impact as well as favourable properties like luminescent, dielectric, semiconductor, catalytic, magnetic, fluorescent, and ion-exchange [2-6]. Rare earth elements have been widely used in luminescence phosphors as activators which play a crucial role in the host phosphor because of their emission color based on 4f–4f and 5d–4f transitions. The strontium pyrophosphate phosphor has been developed to enhance the optical property by the varying different parameters such as synthesis temperature, different doping ions and varying doping concentrations.

OBJECTIVES AND SCOPE OF THE WORK

The major importance of the research work is to synthesis a luminescence phosphor that can give the efficient luminescence and having multiple applications in solid state lighting devices and dosimetry. Inorganic pyrophosphate phosphor was selected as a host material for the obtaining the purpose and trivalent rare earth ions were taken for doping.

To achieve the aim of the research work, the following research objectives were carrying out.

- To synthesis rare earth doped Strontium Pyrophosphate ($Sr_2P_2O_7$) phosphor, high temperature combustion method was taken as synthesis process. The phosphors were synthesized for different concentrations of different doping rare earth ions at temperature 900°C and 1200°C.
- The structural study and phase formation of the synthesize phosphors were accomplished by x-ray diffraction (XRD). The bond formations of the phosphors were characterized by Fourier Transform Infrared spectroscopy (FTIR) and surface morphology was carried out by Scanning Electron Microscopy (SEM).

- The analysis of optical properties of the phosphor was carried out by photoluminescence (PL). The dosimetry property was studied through thermoluminescence (TL) after beta irradiation of the phosphor by Sr^{90} beta source for different doses.

EXPERIMENTAL METHOD

Cerium, Terbium, Europium, Erbium end Gadolinium rare earth doped strontium pyrophosphate samples for different doping concentrations were synthesized by combustion synthesis method at 1200°C temperature. The reactants $SrCO_3$ (A.R.), $(NH_4)_2HPO_4$ (A.R.) and for host and CeO_2 (99.99%) (A.R.), Tb_2O_3 (99.99%) (A.R.), Eu_2O_3 (99.99%) A.R., Er_2O_3 (99.99%) (A.R.), Gd_2O_3 (99.99%) (A.R.) for dopant were taken as per the stoichiometric ratio calculated after chemical equation balancing. Rare earth doped and co-doped strontium pyrophosphate were synthesised for photoluminescence and thermoluminescence studies. All reactants were grinded in an agate mortar for half hour to make homogeneous mixture. The mixture was again grinded with urea (A.R.; 10% of the mass of the mixture), which is taken as a flux in this method to make reaction fast. The mixture was heated in an alumina crucible at 1200°C for 3 hour in a muffle furnace in air and allowed to cool naturally at room temperature. The obtained samples were in the form of a pure white powder form which was again grinded in a mortar-pestle to obtain samples in fine powder form. All samples were prepared for doping concentration 0.1, 0.5, 1.0, 1.5, 2.0, 2.5 and 5.0 mol%.

RESULTS AND DISCUSSION

X-ray diffraction

The XRD pattern of $Sr_2P_2O_7$: 0.5%Ce (x= 0.5, 1.0, 1.5, 2.0, 2.5 mol%) phosphors are shown in Fig.1. Polymorphic $Sr_2P_2O_7$ shows a low-temperature β-phase with a tetragonal structure and a high-temperature α-phase with an orthorhombic structure [1, 7, 8]. The XRD patterns of $Sr_2P_2O_7$ samples were compared with JCPDS standard card no. 24-1011. All peaks observed in prepared samples were significantly matching with the JCPDS data which indicates the existence of a pure single phase α- $Sr_2P_2O_7$. Structural analysis was carried out using powderX software for XRD analysis. The analysis of $Sr_2P_2O_7$ confirms that the sample has a pure α-phase with crystallization in the orthorhombic space group of Pnam. Its lattice constants are a = 8.886 Å, b = 13.102 Å, c = 5.407 Å and volume of unit cell is 629.588 $Å^3$. It can be seen that the doping concentration does not significantly affect the crystal structure of $Sr_2P_2O_7$. The XRD analysis confirms that the desired $Sr_2P_2O_7$ was formed in the pure α-phase using the high-temperature combustion method. Comparative XRD analysis of the sample and the JCPDS file is shown in Table 1.

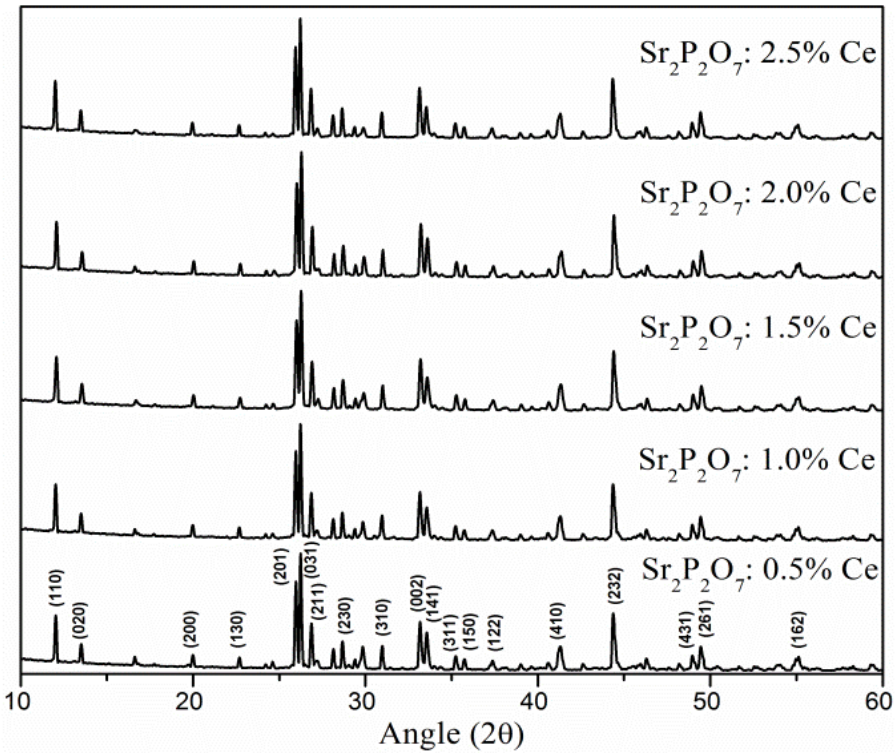

Figure 1. X-ray diffraction pattern of Ce^{3+} doped $Sr_2P_2O_7$ phosphors.

XRD patterns of pure $Sr_2P_2O_7$: Ce^{3+} and JCPDS: 24-1011 are shown in Fig. 1.The XRD patterns of rare earth doped $Sr_2P_2O_7$ samples are compared with JCPDS standard card no. 24-1011. The hkl parameters of the prepared samples are similar to that of the JCPDS standard card no. 24-1011 of α-$Sr_2P_2O_7$ that indicates the existence of a pure single-phase α-$Sr_2P_2O_7$. The structural parameters of the samples were analyzed using powder software for XRD analysis. The analysis confirms that the samples have a pure α-phase with crystallization in the orthorhombic structure and space group of P_{nam}. The doping of various rare earth ions and their percentage concentration does not make any perceptible variation in XRD patterns as well as no other peaks found than that of $Sr_2P_2O_7$ in these patterns. This indicates that the prepared samples are single phased and substitution of Sr^{2+} by RE^{3+} does not cause any substantial modification in the crystal structure of host. Some prominent intense peaks are observed in the XRD patterns at different 2θ values of 12.12°, 25.95°, 26.27°, 26.93°, 33.16°, 33.63° and 44.40° corresponding to the (110), (201), (031), (211), (002), (141) and (232) planes for these host lattice respectively. Sharp intense peaks in the XRD patterns of all rare earth doped samples signify that all samples are polycrystalline material.

The doping of Ce^{3+}, Dy^{3+}, Tb^{3+}, Eu^{3+}, Gd^{3+} do not show any measurable influence on the host $Sr_2P_2O_7$ structure, that can observed from the XRD patterns of respective sample. The reason for this is that ionic radius of doping is much lesser then that of host ion which is replace. The doping ions cannot replace P^{5+} ion but it can easily fit into the site of Sr^{2+} ion as the ionic radius of Ce^{3+} (1.01 Å), Dy^{3+} (0.97 Å), Tb^{3+} (0.923 Å), Eu^{3+} (0.947 Å) and Gd^{3+} (0.937 Å) is smaller than the ionic radius of

Sr^{2+} (1.14 Å) and larger than ionic radius of P^{5+} (0.52 Å). This could be happen because of substitutional doping had been take place on Sr^{2+} lattice site and structural properties remains same in all samples.

JCPDS (24-1011) Data					**Experimental Data $Sr_2P_2O_7$**				
a = 8.917 Å	**b = 13.160 Å**		**c = 5.400 Å**		**a = 8.993 Å**	**b = 13.236 Å**		**c = 5.523 Å**	
V = 633.677 Å^3					**V = 657.648 Å^3**				
2θ	**d**	**h**	**k**	**l**	**$2\theta_{Exp}$**	**d_{Exp}**	**h**	**k**	**l**
11.950	7.400	1	1	0	12.016	7.36	1	1	0
13.404	6.600	0	2	0	13.512	6.548	0	2	0
19.882	4.462	2	0	0	19.962	4.444	2	0	0
22.548	3.940	1	3	0	22.672	3.919	1	3	0
25.886	3.439	2	0	1	25.927	3.434	2	0	1
26.141	3.406	0	3	1	26.210	3.397	0	3	1
26.774	3.327	2	1	1	26.817	3.322	2	1	1
28.018	3.182	1	3	1	28.091	3.173	1	3	1
28.512	3.128	2	3	0	28.636	3.115	2	3	0
30.807	2.900	3	1	0	30.921	2.890	3	1	0
33.152	2.700	0	0	2	33.105	2.704	0	0	2
33.407	2.680	1	4	1	33.509	2.672	1	4	1
35.107	2.554	3	1	1	35.188	2.549	3	1	1
35.524	2.525	1	5	0	35.693	2.514	1	5	0
37.344	2.406	1	2	2	37.351	2.406	1	2	2
44.277	2.044	2	3	2	44.347	2.041	2	3	2
46.133	1.966	4	2	1	46.288	1.960	4	2	1
48.761	1.866	4	3	1	48.957	1.859	4	3	1
49.211	1.850	2	6	1	49.443	1.842	2	6	1
55.114	1.665	0	3	3	55.104	1.665	0	3	3

Table 1. Comparison of experimental XRD data with published JCPDS data.

The XRD pattern of $Sr_2P_2O_7$: 1.0%Ce, 1.0%RE (RE = Dy, Tb, Gd, Er, Eu, Nd, Sm) phosphors are shown in Fig.2. The lattice parameters of all samples for double doping are summarized in Table 2.

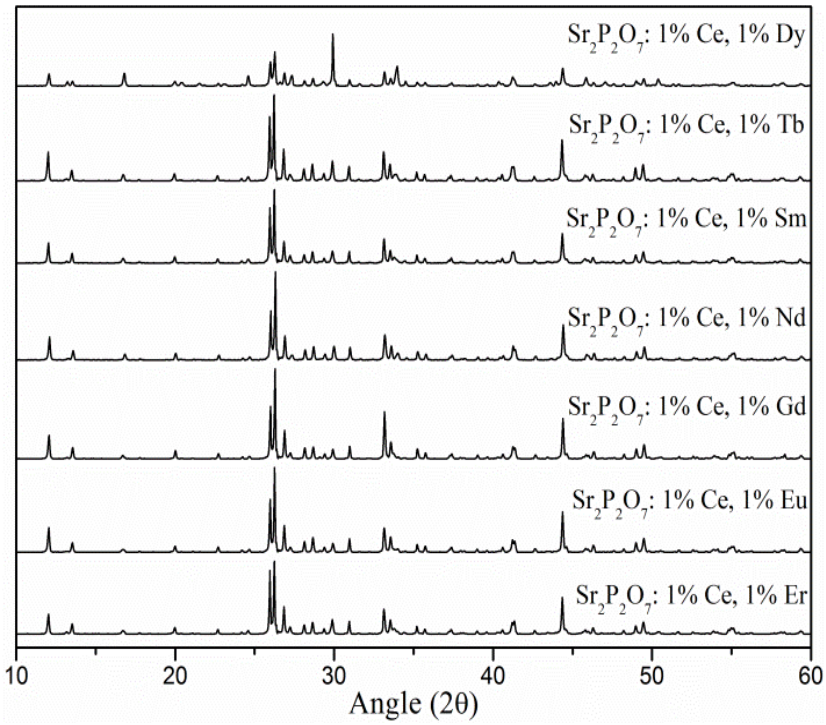

Figure 2. X-ray diffraction patterns of 1% Ce, 1% RE doped $Sr_2P_2O_7$ phosphors.

Sample	Lattice Parameter			Volume of Unit Cell 'V' ($Å^3$)	Crystalline Size (nm)	
	a (Å)	b (Å)	c (Å)		Scherrer's formula	W-H Plot
$Sr_2P_2O_7$: Ce, Eu	8.872	13.177	5.431	634.92	76.39	80.45
$Sr_2P_2O_7$: Ce, Tb	8.858	13.161	5.415	631.28	72.24	73.89
$Sr_2P_2O_7$: Ce, Dy	8.838	13.142	5.409	638.25	71.46	73.12
$Sr_2P_2O_7$: Ce, Er	8.795	13.119	5.375	620.17	67.59	70.67
$Sr_2P_2O_7$: Ce, Gd	8.865	13.168	5.425	633.28	74.74	76.34
$Sr_2P_2O_7$: Ce, Sm	8.879	13.182	5.449	637.77	77.52	79.97
$Sr_2P_2O_7$: Ce, Nd	8.889	13.193	5.460	640.31	79.11	84.85

Table 2. Summary of lattice parameters of double rare earth doped $Sr_2P_2O_7$.

FTIR

IR transmittance spectra were recorded from the KBr pellet of $Sr_2P_2O_7$. The KBr pellet was prepared in a 99 : 1% ratio of KBr to $Sr_2P_2O_7$ total weight at a thickness of 1 mm. Fig.3 shows the IR spectrum for 0.5 mol% Ce-doped $Sr_2P_2O_7$ and Ce-doped $Sr_2P_2O_7$ phosphor in the wavenumber range

from 350–1200 cm^{-1} and 400–1200 cm^{-1}, respectively. The IR spectrum of $Sr_2P_2O_7$ shows characteristic bands at 746 and 1190 cm^{-1} corresponding to the absorption of $(P_2O_7)^{-4}$, which are attributed to the presence of pyrophosphate groups. The intense band at 1047 cm^{-1} is assigned to the antisymmetric stretching mode of (P–O). The intense broad peak at 976 cm^{-1} is due to the symmetric stretching mode of (P–O). The shoulder peaks at 612 and 620 cm^{-1} are attributed to the bending mode components of (O–P–O) [9]. The intense peaks observed in range 450–750 cm^{-1} correspond to the antisymmetric bending modes of PO_4, whereas the peaks between 950 and 1200 cm^{-1} are due to the stretching modes of PO_4 [10]. The characteristic IR bands observed at positions 976, 1014, 1047, 1062 and 1109 cm^{-1} are assigned to the antisymmetric stretching mode of the P–O bond of $(PO_4)^{-3}$ groups in $Sr_2P_2O_7$. The bands at 547, 562, 612 and 620 cm^{-1} are assigned to the antisymmetric bending vibration of $(PO_4)^{-3}$ groups. The characteristic bands that exist in the IR spectrum indicate the presence of phosphate group vibrations in α- $Sr_2P_2O_7$ [11, 12]. The IR spectra of α- $Sr_2P_2O_7$ for different concentrations of Ce are shown in Fig. 7 indicate that the Ce concentration does not affecting the bond stretching in α- $Sr_2P_2O_7$ and that there is a single α-phase of $Sr_2P_2O_7$.

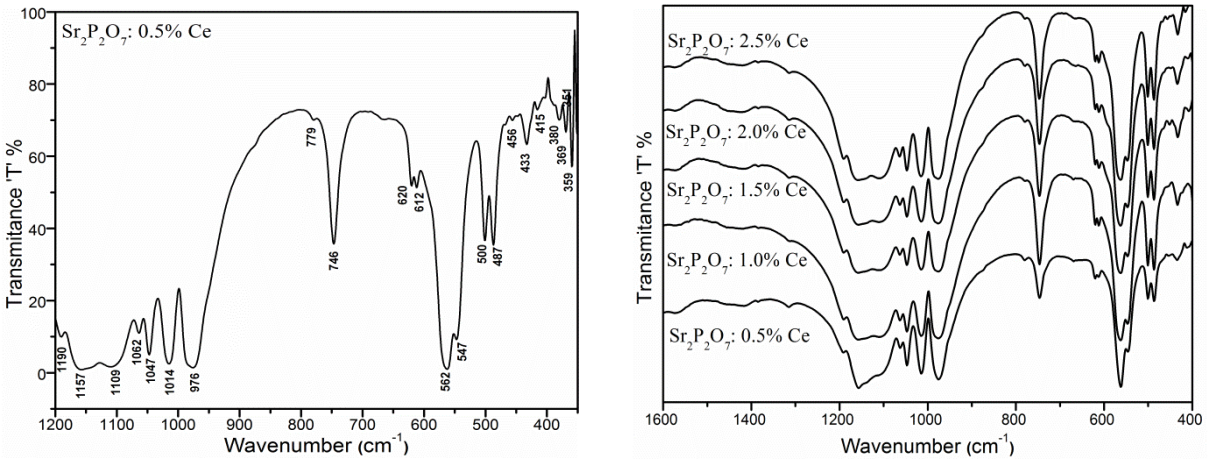

Figure 3. FTIR spectra of Ce doped $Sr_2P_2O_7$ phosphors.

The FTIR spectra of Dy doped $Sr_2P_2O_7$, Tb doped $Sr_2P_2O_7$, Eu doped $Sr_2P_2O_7$, Er doped $Sr_2P_2O_7$ and Ce, RE doped $Sr_2P_2O_7$ samples are very similar with respect to the Ce doped $Sr_2P_2O_7$. This could be the reason for no change in the structural formation of host after doping. All result obtained from FTIR spectra are consistent and significant.

Photoluminescence

The PL excitation spectrum of Ce-doped α-$Sr_2P_2O_7$ phosphor shown in Fig. 4(a) was recorded at room temperature (RT). It shows two broad intense peaks at 268 and 310 nm, as well as a shoulder peak around 254 nm. The broad absorption bands are due to the higher energy, which allowed 4f–5d transitions in trivalent cerium ions, Ce^{3+}. PL emission spectra for Ce-doped α-$Sr_2P_2O_7$ phosphor are shown in Fig. 4(b), (c), (d) for different excitation wavelengths. Ce-doped α-$Sr_2P_2O_7$ phosphor exhibits high luminescence and a maximum emission band centred at 385 nm. The variation in the intensity of the PL emission depended on the excitation energy and the concentration

of cerium. Gaussian fitting of the PL emission spectra of the Ce-doped α-$Sr_2P_2O_7$ phosphor revealed that the emission originates from the 5d–4f transition of Ce^{3+}. Each PL emission spectrum of Ce-doped α-$Sr_2P_2O_7$ phosphor consists of two Gaussian peaks at 363 and 395 nm in the near-UV region. The observed doublet Gaussian bands are due to the allowed transitions from the relaxed lowest 5d excited state to the $^2F_{5/2}$ and $^2F_{7/2}$ ground states of Ce^{3+} ions. The $4f^1$ ground state yields two levels $^2F_{5/2}$ and $^2F_{7/2}$ due to the spin-orbit coupling of 4f. The energy discrepancy between the two Gaussian emission bands, the first at 363 nm (27,397 cm^{-1}) and the second at 395 nm (25,316 cm^{-1}) is about 2081 cm^{-1} [13, 14]. The broad PL emission band is due to the lowest crystal field component of the $5d^1$ configuration to the two distinct levels of ground state. The observed Stokes shift is mainly due to the ideal spectroscopic characteristics of Ce^{3+} and the ability to incorporate Ce^{3+} into the host material.

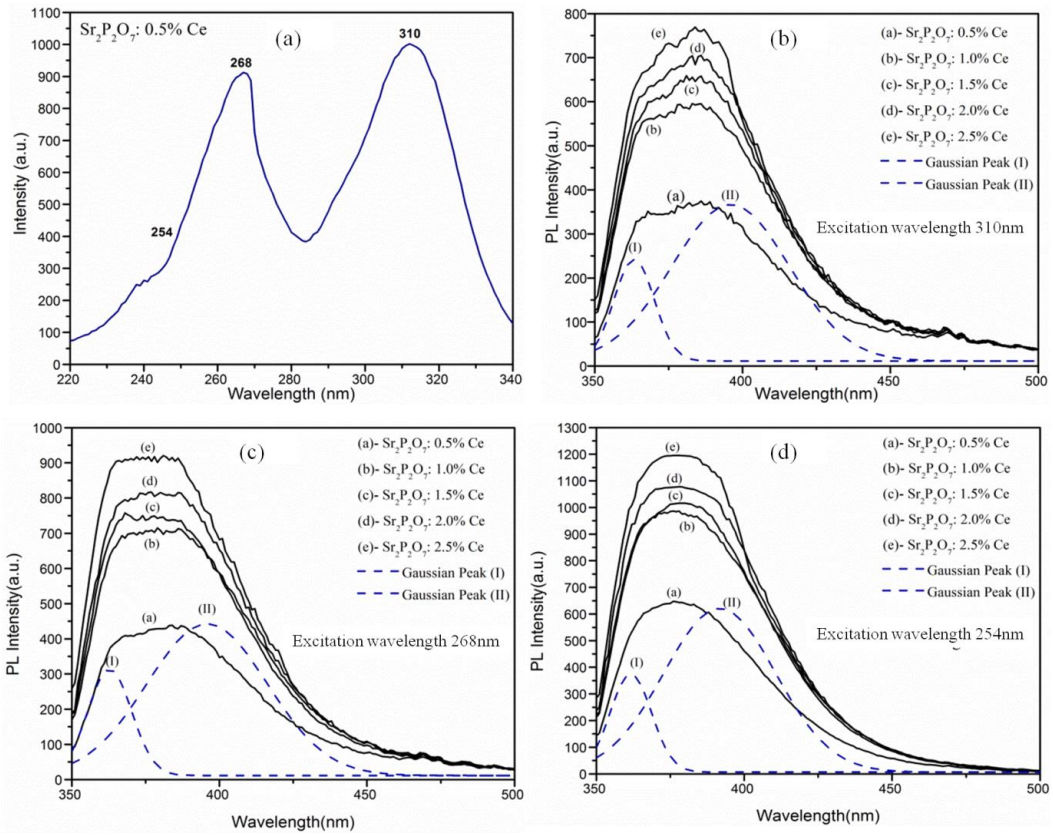

Figure 4. PL excitation and emission spectra of Ce doped α-$Sr_2P_2O_7$ phosphors.

Fig. 5(a) shows excitation spectrum of Tb^{3+} doped α-$Sr_2P_2O_7$ phosphor monitored at 545 nm emission wavelength. The excitation spectra exhibits a single band peaked at 232 nm due to the $4f^8$ – $4f^75d^1$ (f – d) transition of Tb^{3+}. An excitation band illustrate that the phosphor can be excited through the UV ligth about 232 nm. Fig. 5(b), illustrates the PL emission spectra, recorded by exciting the samples at their optimized excitation wavelength (i.e, 232nm) to determine the PL emission from samples. It is important to find out the detailed information of the nature of the Tb^{3+} luminescence centre form inside host lattice. The emission spectra does not give all information about luminescence centre, due to the high degeneracy of the Tb^{3+} levels involved in several transitions.

The PL emission spectra of the Tb^{3+} doped α-$Sr_2P_2O_7$ shows peaks at 415, 436, 469, 491, 545 and 584 nm as a consequence of the characteristics radiative transitions of Tb^{3+} ion. All defined transitions occurring are corresponds to the $^5D_3$–$^7F_5$, $^5D_3$–$^7F_4$, $^5D_3$–$^7F_3$, $^5D_4$–$^7F_6$, $^5D_4$–$^7F_5$ and $^5D_4$–$^7F_4$, respectively [15]. The observed high intense peak at 545 nm can be attributed to green emission which is characteristic emission of Tb^{3+}. Tb^{3+} ion replace the host Sr^{2+} ion from lattice site without any structural deformation, which is mainly responsible for contraction of unit cell of host $Sr_2P_2O_7$.

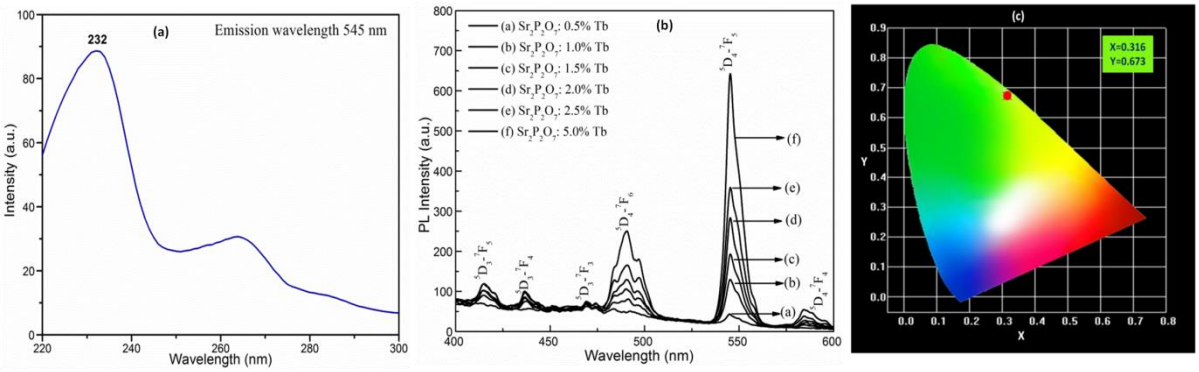

Figure 5. (a) PL excitation spectra, (b) PL emission spectra, (c) CIE diagram.

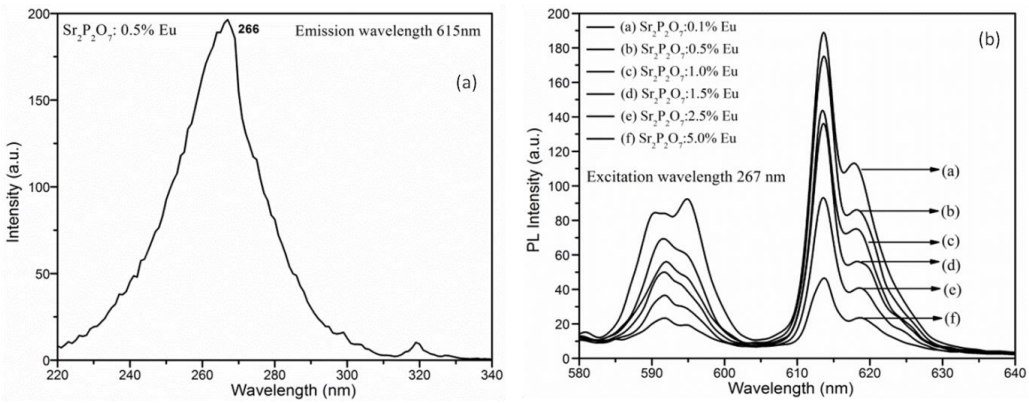

Figure 6. (a)PL excitation spectra, (b)PL emission spectra of Eu doped α-$Sr_2P_2O_7$ phosphors.

The excitation spectrum from 220 to 340 nm of Eu doped α-$Sr_2P_2O_7$ monitored at 616 nm is shown in Fig. 6(a). There is a broad absorption band in the wavelength range 220–300 nm, which originates from the charge-transfer transition from the filled 2p shell of O^{2-} to the partially filled 4f shell of Eu^{3+}. In the excitation spectrum, the absorption peak at 267 nm is the strong peak, corresponding to this wavelength emission spectra were recorded. Fig. 6(b) presents the emission spectrum of Eu doped α-$Sr_2P_2O_7$ excited at 267 nm in the wavelength of 580–640 nm. There are two typical emission bands observed around 585 and 616 nm assigned to the $^5D_0$ – $^7F_1$ and $^5D_0$ – $^7F_2$ transitions of Eu^{3+}, respectively.

Rare earth co-doped $Sr_2P_2O_7$ phosphor gives the characteristic PL emissions of the doping ion in the visible region of electromagnetic wave spectrum.

Thermoluminescence

Fig. 7(a) shows a typical glow curve of Ce doped α-$Sr_2P_2O_7$ phosphor for 4°K/s heating rate after irradiation of x-ray during x-ray diffraction characterization. The TL intensity of glow curve is prominent at 192°C for different concentrations of Ce doping. It is found that intensity of TL peak decrease with increase in Ce concentration. The thermoluminescence analysis of the glow peaks were done by initial rise method, peak shape method and heuristic method. Glow curve kinetic parameters like activation energy 'E_a', frequency factor 's', order of kinetics were calculated using different TL analysis methods. Fig. 7(b) shows the ln (I) Vs 1/T graph for intial rise method to evaluated activation energy 'E_a' and frequency factor 's' of TL glow curves.

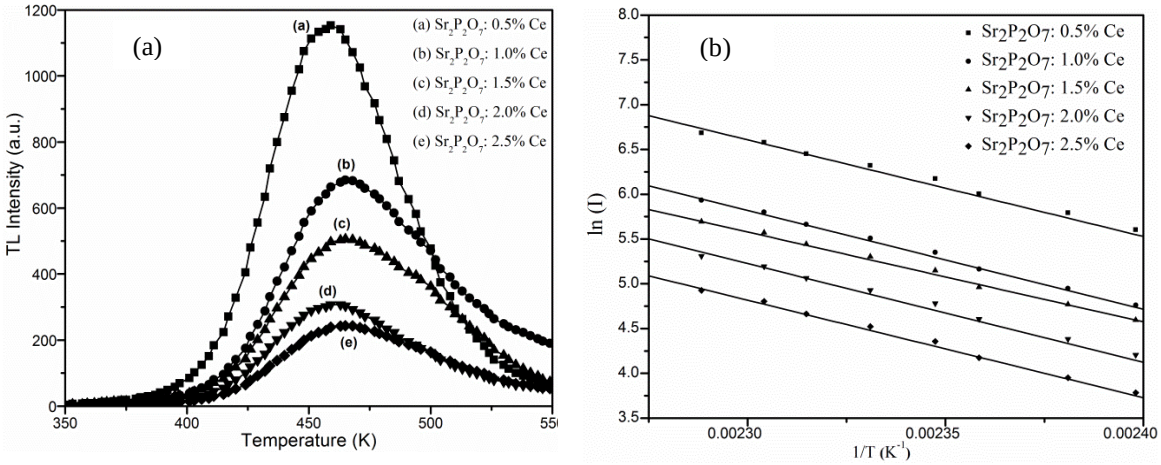

Figure 7. (a) TL Glow curves, (b) TL analysis of glow curves by Initial rise method of Ce doped α-$Sr_2P_2O_7$ phosphors after X-ray irradiation.

The Glow curve parameters calculated for peak shape method were illustrated in Table 3. The activation energy 'E_a' of the glow curve calculated from different method is lying in the range of 0.85-1.11eV which is mentioned in Table 4. The frequency factor measured by initial rise method was about 10^{13}-$10^{14}s^{-1}$.

Sample		δ		μ_g	$c_\gamma(\tau)$	$c_\gamma(\delta)$	$c_\gamma(\omega)$	$b_\gamma(\tau)$	$b_\gamma(\delta)$	$b_\gamma(\omega)$
$Sr_2P_2O_7$: 0.5% Ce	29.5	35.5	65	0.54	1.89	1.9	3.81	2.11	0	1
$Sr_2P_2O_7$: 1.0% Ce	30	49	79	0.52	2.11	2.44	4.56	2.42	0	1
$Sr_2P_2O_7$: 1.5% Ce	32	49	81	0.53	2.06	2.33	4.41	2.36	0	1
$Sr_2P_2O_7$: 2.0% Ce	32	39	71	0.54	1.9	1.92	3.84	2.12	0	1
$Sr_2P_2O_7$: 2.5% Ce	31	47.5	78.5	0.52	2.06	2.33	4.41	2.36	0	1

Table 3. The calculated constants of peak shape method for measuring activation energy.

Sample	Activation Energy (eV)							Frequency Factor (s^{-1}) by IR Method
	Initial Rise method	Alternative method (IR)	Peak Shape method			Peak Position Method		
			E_τ	E_δ	E_ω	$T_m/500$	$23kT_m$	
$Sr_2P_2O_7$: 0.5% Ce	0.93±0.02	1.03±0.05	0.99±0.29	0.97±0.20	0.98±0.12	0.92±0.01	0.91±0.01	1.79×10^{14}
$Sr_2P_2O_7$: 1.0% Ce	0.95±0.01	1.02±0.05	1.07±0.28	0.93±0.14	0.99±0.10	0.93±0.01	0.92±0.01	1.43×10^{14}
$Sr_2P_2O_7$: 1.5% Ce	0.86±0.01	1.01±0.05	1.01±0.25	0.88±0.13	0.93±0.09	0.93±0.01	0.92±0.01	1.13×10^{13}
$Sr_2P_2O_7$: 2.0% Ce	0.95±0.02	1.03±0.05	0.93±0.25	0.91±0.17	0.92±0.10	0.92±0.01	0.91±0.01	7.75×10^{13}
$Sr_2P_2O_7$: 2.5% Ce	0.94±0.01	1.02±0.05	1.05±0.27	0.91±0.14	0.97±0.09	0.93±0.01	0.92±0.01	3.65×10^{13}

Table 4. Activation energy and frequency factor for glow curve of Ce doped α-$Sr_2P_2O_7$.

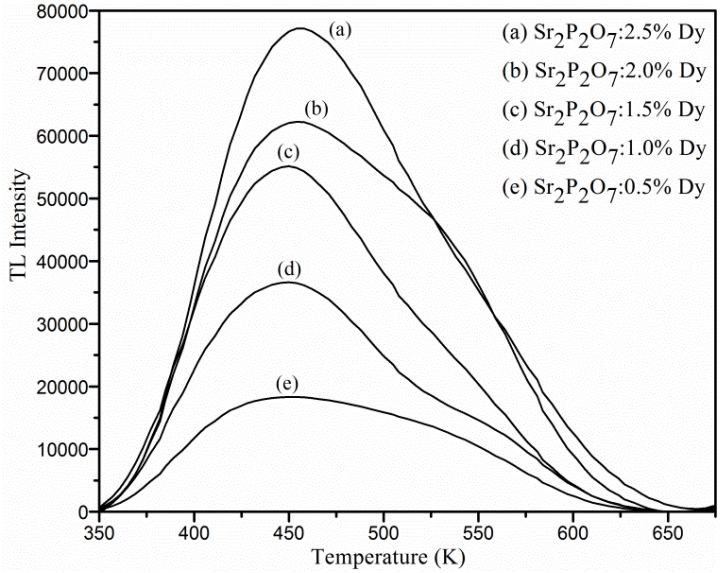

Figure 8. TL Glow curves of Dy doped α-$Sr_2P_2O_7$ phosphors after X-ray irradiation.

The TL glow curves of β-irradiate Dy doped α-$Sr_2P_2O_7$samples were shown in Fig. 8 recorded at 6 K/s heating rate. It was observed that the broad glow curve of samples exhibited one strong peak at around 180–182°C. The intensity of TL count was increase with increase in concentration of Dy doping. The kinetic parameters of the glow curve were calculated by initial rise method TL analysis. The summary of calculated TL parameters of the Dy doped α-$Sr_2P_2O_7$ phosphors is illustrated in Table 5.

Sample	Activation Energy 'E_a' (eV) and Frequency Factor 's' (s^{-1})			
	IR Method (eV)	Frequency Factor (s^{-1})	Peak Position Method (eV)	
$Sr_2P_2O_7$: 0.5% Dy	1.07±0.02	6.80×10^{18}	0.91±0.01	0.90±0.01
$Sr_2P_2O_7$: 1.0% Dy	1.06±0.03	7.74×10^{18}	0.90±0.01	0.89±0.01
$Sr_2P_2O_7$: 1.5% Dy	1.08±0.02	2.52×10^{18}	0.90±0.01	0.89±0.01
$Sr_2P_2O_7$: 2.0% Dy	1.01±0.02	1.63×10^{18}	0.91±0.01	0.90±0.01
$Sr_2P_2O_7$: 2.5% Dy	1.02±0.01	2.05×10^{18}	0.91±0.01	0.90±0.01

Table 5. Activation energy 'E_a' and frequency factor 's' of TL glow curves of Dy doped α-$Sr_2P_2O_7$ phosphors.

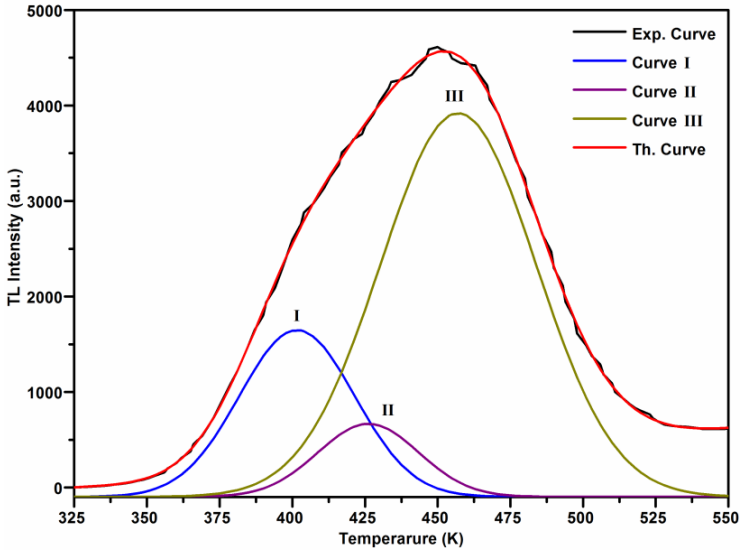

Figure 9. Glow curve fitting of $Sr_2P_2O_7$:0.5%Er phosphor irradiated with 50Gy beta dose.

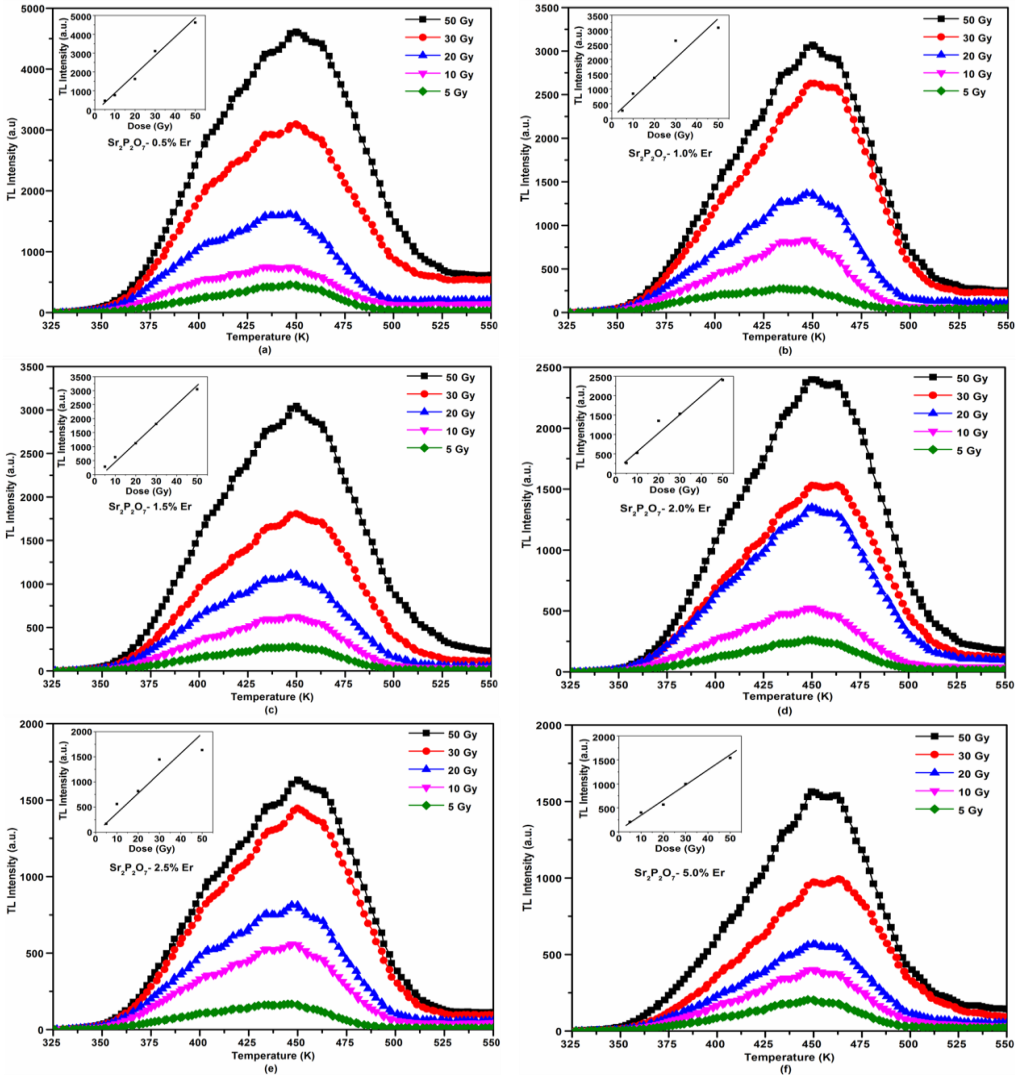

Figure 10. TL glow cures of β-irradiated samples (a) $Sr_2P_2O_7$: 0.5%Er; (b) $Sr_2P_2O_7$: 1.0%Er; (c) $Sr_2P_2O_7$: 1.5%Er; (d) $Sr_2P_2O_7$: 2.0%Er; (e) $Sr_2P_2O_7$: 2.5%Er; (f) $Sr_2P_2O_7$: 5.0%Er.

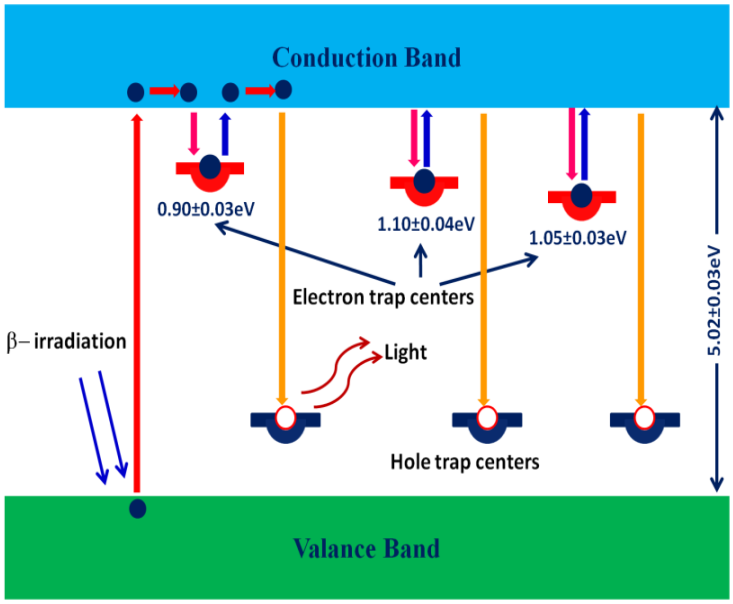

Figure 11. TL mechanism and energy level diagram of Er^{3+} doped $Sr_2P_2O_7$ phosphor.

Fig. 10 shows TL glow curves measured at 6 K/s from the samples of Er^{3+} doped $Sr_2P_2O_7$ after β-irradiation and inserted graph shows the dose response of each samples. To reveal the existence of trap centers generated in energy gap by doping ions, a method of glow curve deconvolution of TL glow curve was carried out. Fig. 9 shows the curve fitting for sample $Sr_2P_2O_7$: 0.5%Er irradiated with 50 Gy beta dose with best fitting parameter. The curve fitting analyses of TL glow curves revealed that three peaks are present in glow curve at different temperatures located at 400 K, 430 K and 464 K corresponds to the three trap centers formed at different depths. The complex nature of the TL glow curves could be attributed because of the overlapping of various bands present at a close distribution of their trap depths. All fitted curves of TL glow curve was analyzed by Peak shape method alternatively called Chen's method to find out the kinetic parameters in order to understand the basic mechanisms involved in the emission. The average activation energy 'E_a' calculated to be 0.90±0.03 eV, 1.10±0.04 eV and 1.05±0.03 eV for the peak I, peak II and peak III, respectively. The frequency factors 's' for various depths are 1.5×10^{11} s^{-1}, 9.5×10^{12} s^{-1} and 1.1×10^{11} s^{-1}, respectively. The order of kinetics 'b' was determined from the geometric shape factor 'μ_g'. The suggested values of geometric factor are 'μ_g=0.42 and 0.52 for first and second order kinetics, respectively. It is found that geometric factor for different peaks were nearer to 0.52 which revealed that the glow curve having second order kinetics. Activation energy of the glow curve gives the information about the trap depth located in energy gap. Fig. 11 shows the TL mechanism of Er^{3+} doped $Sr_2P_2O_7$ phosphor. The TL mechanism explains the electron excitation with β–irradiation, Electron trapping and recombination of electron by emitting light at time of heating. The kinetic parameters calculated from above mentioned method are given in Table 6.

Peak	Tm (K)	T (K)	δ (K)	ω (K)	μ_g	Activation Energy 'E_a'			Frequency factor 's' (s^{-1})	Order of Kinetics 'b'
						E(τ) eV	E(ω) eV	E(δ) eV		
Peak I	400	24	25	49	0.51	0.89±0.03	0.91±0.04	0.90±0.03	1.5×10^{11}	2
Peak II	430	23	25	48	0.52	1.10±0.05	1.11±0.04	1.10±0.03	9.5×10^{10}	2
Peak III	464	27	25	52	0.49	1.05±0.03	1.05±0.03	1.04±0.04	1.1×10^{11}	≈2

Table 6. Activation energy 'E_a', frequency factor 's' and order of kinetics 'b' of the TL glow curve of sample $Sr_2P_2O_7$:0.5%Er after deconvolution curve fitting technique.

Fig. 12 shows the TL glow curve of Eu doped $Sr_2P_2O_7$ for various dose, it shows there is no major change in the shape of TL glow curve and peak position glow curve. The insert graphs in Fig. 12 gives the information about the dose response for β-dose 5Gy to 50Gy; it indicates that TL intensity is linearly varied with dose of irradiation. TL intensity of β-irradiated phosphor has been considerably influenced by doping concentrations and the dose given to the phosphor. The variation in TL intensity with doping concentration of Eu^{3+} for 0.1mol% to 5.0mol% in host $Sr_2P_2O_7$ was studied for dose 5Gy to 50Gy of β-irradiated. By knowing the trapping parameters like order of kinetics 'b', trap-depth or activation energy 'E_a' and frequency factor 's' of glow curve, the TL phenomenon occurred in phosphor have been evaluated.

Fig. 13 shows the TL mechanism of Eu doped $Sr_2P_2O_7$. In this study Eu^{3+} ions were doped as impurity ion which could be incorporated in cation Sr^{2+} site. Because of ionic radius of Eu^{3+} ion is around 0.947Å which is greater than that of the ionic radius of P^{5+} (0.52Å) and less than that of the ionic radius of Sr^{2+} (1.14Å). The reason could be the good agreement of substitutional incorporation. TL study of all phosphors with different doping concentration revealed that the localized energy level formed in forbidden gap at same energy but the population of electron traps was changed with impurity concentration.

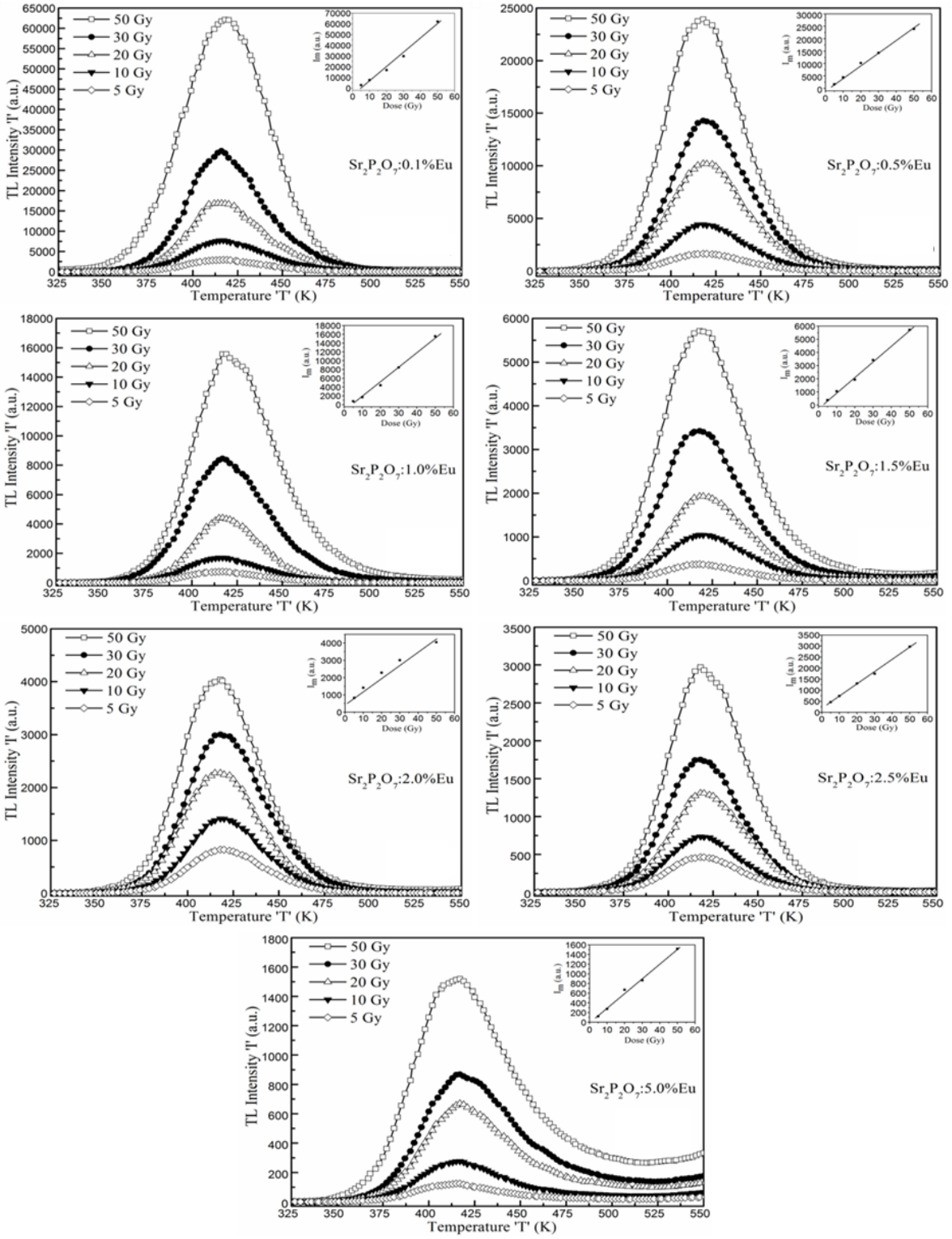

Figure 12. TL glow curves of Eu doped $Sr_2P_2O_7$ phosphors for different dose of β-irradiation.

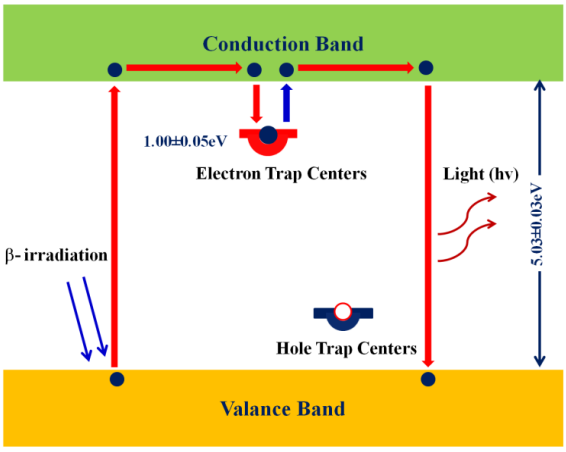

Figure 13. Electronic transitions occurred in TL mechanism of Eu doped $Sr_2P_2O_7$.

It is observed that TL count for lower concentration of Eu^{3+} ion is higher than that of higher concentration. It infers that for lower concentration of impurity ion substitutional incorporation is higher than that of higher concentrations. This implies that higher the substitution provide higher electron trap and hence the TL intensity increases. TL parameter obtained using different methods with statistical significance are very similar and reliable. The results obtained reveal that the curve having second order kinetics. Activation energy calculated from different methods is lies in the range (0.95±0.05) eV to (1.05±0.05) eV. Frequency factor is lies in the range 10^{10} to $10^{11}s^{-1}$.

CONCLUSION

Rare earth doped $Sr_2P_2O_7$ phosphor synthesized by combustion method have pure α-phase with an orthorhombic crystal structure. FT-IR gives good agreement for the bond structure of $Sr_2P_2O_7$ because FTIR spectra of all samples having same spectral formation. Doping concentration also does not affect the structural properties of the host because of substitutional doping.

Ce-doped $Sr_2P_2O_7$ shows predominant PL intensity in the UV region, which is mainly dependent on the excitation wavelength and the concentration of Ce, the maximum emission of PL intensity is observed at 254 nm excitation and 2.5 mol% Ce. Tb^{3+} doped α-$Sr_2P_2O_7$ doped with 5.0 mol% Tb^{3+} shows excellent green emission for a given excitation and this material has potential to be used as a green luminescent material for display systems in solid state lighting applications. Eu-doped $Sr_2P_2O_7$ phosphor gives intense red emission revealed that phosphor has potential application as red phosphor in LED applications.

The TL glow curve of Ce-doped $Sr_2P_2O_7$ phosphor shows a stable single glow peak at 192°C, the activation energy was calculated to be in the range 0.85–1.1 eV for a frequency factor of 10^{13} – 10^{14} s^{-1} for X-ray irradiation. Excellent TL properties of phosphor reveal its wide application radiation dosimeters. TL of glow curve of Tb-doped $Sr_2P_2O_7$ after β-irradiation reveal that the TL glow curve has two peaks analogous to traps created within band structure of host because of Tb^{3+} doping. The

calculated parameters of the glow curve imply that it is of second order kinetic. The activation energy 'E_a' and frequency factor 's' are of the order of 0.8–0.9eV and 1×10^{9}–1×10^{11} s^{-1} for the curve with maximum temperature of around 420 K, respectively, and of the order of 0.5–0.6eV and 1×10^{6}–$1\times10^{7}s^{-1}$ for the curve with maximum temperature of 525K. TL parameters suggest phosphor as a good TL material. TL investigations of Er^{3+} doped $Sr_2P_2O_7$ phosphor after β-irradiation the dose response of intense peak at 451 K is linear for dose range 5 Gy to 50 Gy. Low fading of TL intensity and multiple time reusability of phosphors gives its potential properties for TLD phosphor. Activation energy and the frequency factor calculated from the analysis are favourable for proposing this phosphor for dosimetric applications. TL glow curve of Eu doped $Sr_2P_2O_7$ phosphor after β-irradiation having symmetric bell shape nature with peak temperature 418K. Measured parameters reveals that the glow curves have second order kinetics. Activation energy calculated using different method is lying between the ranges 0.90 eV to 1.10 eV. Frequency factor is lying between range 10^{10} to $10^{11}s^{-1}$. TL sensitivity, fading rate and linear dose response of the phosphors are excellent. The kinetic parameters obtained from all analysis methods gives good agreement of TLD application.

References

1. G. Blasse and B.C. Grabmaier, Luminescent Materials, Springer-Verlag, Berlin, 1994.
2. M. Gaft, R. Reisfeld, G. Panczer, Modern Luminescence Spectroscopy of Minerals and Materials, Springer-Verlag Berlin Heidelberg 2005.
3. D. Hou, B. Han, W. Chen, H. Liang, Q. Su, Pi. Dorenbos, Y. Huang, Z. Gao, Y. Tao, *Journal of Applied Physics*, 108, 2010, 083527.
4. V. Natarajan, M. K. Bhide, A. R. Dhobale, S.V. Godbole, T.K. Seshagiri, A.G. Page, Chung-Hsin Lu, *Materials Research Bulletin*, 39, 2004, 2065.
5. A. N. Yazici, S. Seyyidoglu, H. Toktamisa, A. Yilmaz, *Journal of Luminescence*, 130, 2010, 1744.
6. Z. Hao, J. Zhang, X. Zhang, X. Sun, Y. Luo, S. Lu, *Applied Physics Letters*, 90, 2007, 261113.
7. Z. Hao, J. Zhang, X. Zhang, S. Lu, Y. Luo, X. Ren, X. Wang, *Journal of Luminescence*, 128, 2008, 941.
8. R. Kohale, S. J. Dhoble, *Search & Research*, 2(2), 2011, 16.
9. S. C. Liou, S. Y. Chen, J. S. Bow, *Biomaterials*, 25, 2004, 189–96.
10. M. T. P. Ledent, *Journal of Solid State Chemistry*, 23, 1978, 147–54.
11. N. Khay, A. Ennaciri, M. Harcharras, *Vibrational Spectroscopy*, 27, 2007, 119–26.
12. R. Velchuri, B. Vijaya Kumar, V. Rama Devi, D. Jaya Prakash, M. Vithal, *Spectroscopic Letters*, 44, 2011, 258–66.
13. M. R. Lin, W. Liu, H.H. Chen, X. X. Yang, Z. B Wei, D.H. Cao, *European Journal of Inorganic Chemistry*, 23, 2003, 4693–6.
14. D. Wisniewski, A. J. Wojtowicz, W. Drozdowski, J. M. Farmer, L. A. Boatner, *Journal of Alloy Compounds*, 380, 2004, 191–5.
15. L. Song, P. Du, Q. Jiang, H. Cao, J. Xiong, *Journal of Luminescence*, 150, 2014, 50–54.

Brief Information of Proposed Chapters of Thesis

Chapter 1. Introduction

In this chapter, the basic concept of the luminescence phenomenon involved in the phosphor material will be discussed. The literature review of the pyrophosphate materials with its brief information of its phosphor application in luminescence will be explained. It will also contain some overview of strontium pyrophosphate phosphors and the purpose of this research.

Chapter 2. Experimental Method

In this chapter, the synthesis experimental method adopted for the synthesis of the desire phosphor will explained. This chapter also contain the principle and advantages of the synthesis method. The sample preparation of the rare earth doped strontium pyrophosphate by varying some parameters like temperature, concentrations of doping, etc will discussed.

Chapter 3. Structural Characterization

In this chapter, the instrumentation of the characterization techniques will be explained with its principle involved in material characterization. It will contain the results of characterization of the prepared material with its detail discussion.

Chapter 4. Photoluminescence of Rare Earth doped Strontium Pyrophosphate

In this chapter, the instrumentation of photoluminescence (PL) will be discussed. The PL results of the single rare earth doped and double rare earth doped strontium pyrophosphate will be explained with detailed discussion of the photoluminescence properties. It will contain brief explanation of the potential application of the prepared phosphors.

Chapter 5. Thermoluminescence of Rare Earth doped Strontium Pyrophosphate

In this chapter, the instrumentation of thermoluminescence (TL) will be explained. This chapter contains the theoretical background of the TL mechanism and brief information of the analytical methods developed for the TL glow curve analysis. The TL results obtained for the single rare earth doped and double rare earth doped strontium pyrophosphate will be explained on the basis of the TL phenomenon involved in the phosphor. The applications of the prepared phosphors for TL dosimetry will be discussed in this chapter.

Chapter 6. Summary and conclusions

In this chapter, the brief summary of the information of the outcome of the results and discussion will be explained. It will contain brief point of view of this research regarding to the result obtained and the application of the prepare strontium pyrophosphate phosphor.

PROPOSED PLAN OF THESIS CHAPTERS

Chapter 1: Introduction

Chapter 2 Experimental Method

Chapter 3 Structural Characterization

Chapter 4 Photoluminescence of Rare Earth doped Strontium Pyrophosphate

Chapter 5 Thermoluminescence of Rare Earth doped Strontium Pyrophosphate

Chapter 6 Summary and conclusions

LIST OF PUBLICATIONS BASED ON THE RESEARCH WORK

Publications in Refereed Journals

1. **Nimesh P. Patel**, Verma Vishwnath, Dhaval Modi and K. V. R. Murthy and M. Srinivas, Thermoluminescence kinetic features of Eu^{3+} doped strontium pyrophosphate after beta irradiation, ***RSC Advances***, 2016, **6**, 77622-28.
2. **Nimesh P. Patel**, M. Srinivas, Verma Vishwnath, Dhaval Modi and K. V. R. Murthy, Investigation of dosimetric features of beta – irradiated Er^{3+} doped strontium pyrophosphate, ***Advanced Materials Letters***, 2016, **7(6)**, 497-500.
3. **Nimesh P. Patel**, M. Srinivas, Dhaval Modi, Verma Vishwnath and K. V. R. Murthy, Optimization of luminescence properties of Tb^{3+}-doped α- $Sr_2P_2O_7$ phosphor synthesized by combustion method, ***Rare Metals***, 2016, **DOI** 10.1007/s12598-015-0688-x.
4. **Nimesh P. Patel**, M. Srinivas, Dhaval Modi, Verma Vishwnath and K. V. R. Murthy, Luminescence study and dosimetry approach of Ce on an α-$Sr_2P_2O_7$ phosphor synthesized by a high-temperature combustion method, ***Journal of Biological and Chemical* Luminescence**, 2015, 30(4), 472-478.

Presentations in Conferences

1. **Nimesh P. Patel**, M. Srinivas, Verma Vishwnath and Dhaval Modi, The effect of Tb^{+3} on α-$Sr_2P_2O_7$ phosphor for green LED phosphor application, *AIP Conference Proceedings*, 2015, 110017-1-3.
2. **Nimesh P. Patel**, M. Srinivas, Vishwnath Verma, Dhaval Modi and K. V. R. Murthy, Synthesis and Thermoluminescence Dosimetry application of Dy^{+3} activated $Sr_2P_2O_7$, *International Journal of ChemTech Research*, 2014, **6(3)**, 1708-1711.